Received: 10 March 2021 | Revised: 29 June 2021 | Accepted: 2 July 2021

DOI: 10.1002/ajmg.a.62433

CLINICAL REPORT

AMERICAN JOURNAL OF medical genetics PART A WILEY

Low-level mosaicism in tuberous sclerosis complex in four unrelated patients: Comparison of clinical characteristics and diagnostic pathways

Héctor Hugo Manzanilla-Romero[1] | Denisa Weis[2] | Simon Schnaiter[1] | Sabine Rudnik-Schöneborn[1]

[1]Institute of Human Genetics, Medical University of Innsbruck, Innsbruck, Austria

[2]Institute of Medical Genetics, Kepler University Hospital, Johannes Kepler University, Linz, Austria

Correspondence
Sabine Rudnik-Schöneborn, Institute of Human Genetics, Medical University Innsbruck, Peter-Mayr-Str. 1, 6020 Innsbruck, Austria.
Email: sabine.rudnik@i-med.ac.at

Abstract

Tuberous sclerosis complex (TSC) is an autosomal dominant neurocutaneous syndrome caused by either *TSC1* or *TSC2* gene mutations. About 15% of TSC patients remain without genetic diagnosis by conventional analysis despite clinical evidence. It is important to identify somatic mosaics, as therapeutic options are now available in patients with *TSC1* or *TSC2* mutations. Here, we describe the clinical and genetic characteristics of four male TSC patients with low-level mosaicism. Patients presented at ages between 9 months and 32 years. Clinical manifestations varied considerably and included brain lesions in all four patients, cardiac rhabdomyomas in two young patients, skin involvement in two patients, and retinal hamartomas and renal angiomyolipomas in three patients. One patient presented with epileptic seizures and psychomotor delay. Low levels of mosaicism for *TSC1* or *TSC2* mutation were found in different tissue samples employing next generation sequencing and multiple ligation-dependent probe amplification. The five disease-associated variants, including one second-hit mutation, include three truncating mutations and one deletion in *TSC2*, and one truncating mutation in *TSC1*. Sanger sequencing, allele-specific oligonucleotide PCR (ASO-PCR), and droplet digital PCR were used to confirm and quantify the disclosed mutations. Genetic identification of low-level mosaicism for TSC remains challenging but is important for optimal surveillance and management.

KEYWORDS
genetic diagnosis, next generation sequencing, somatic mosaicism, tuberous sclerosis complex

1 | INTRODUCTION

Tuberous sclerosis complex (TSC) is an autosomal dominant genetic disorder characterized mainly by the development of benign tumors in practically any organ including neurological, renal, and dermatological manifestations. The genes implicated in the pathophysiology are *TSC1* and *TSC2* which encode for hamartin and tuberin, respectively, two proteins involved in the mechanistic target of rapamycin (mTOR) pathway. Sporadic cases represent 70% of the TSC population. The disease has a complete penetrance and clinical manifestations appear in an age-related manner (Curatolo et al., 2008). In the past years, it was found that mosaicism can explain up to 58% of

patients who met clinical criteria for TSC but had negative genetic test results in DNA samples extracted from peripheral blood (Tyburczy et al., 2015).

The purpose of this article is to describe the clinical characteristics and the chronologic diagnostic procedures of four patients with low-level mosaicism for TSC followed up at our institutions.

2 | METHODS

2.1 | Next generation sequencing

Massive parallel sequencing: Target gene enrichment from genomic DNA using Nextera® Rapid Capture (TruSight Hereditary Cancer Panel, Illumina) and subsequent massive parallel sequencing (MiSeq, Illumina). Alignment of the sequences to the human reference sequence GRCh37 (hg19) and subsequent data analysis with SeqNext software (JSI). Quantitative analysis of the sequence data with respect to copy number variations (CNV = deletion/duplication) was additionally performed with the CNV Detective Software (Institute for Bioinformatics, JKU Linz; Povysil et al., 2017).

Analyzed target genes: *TSC1* (NM_000368.4) und *TSC2* (NM_000548.3). All coding exonic and flanking intronic sequences (±30 nucleotides) of these genes were sequenced with at least 30-fold coverage. The nucleotide positions are numbered according to the recommendations of the Human Genome Variation Society (den Dunnen & Antonarakis, 2001), in which the A of the start codon ATG represents nucleotide position 1. To detect mosaic mutations, all variants with a frequency greater than 1% in the sequences were assessed and evaluated. The classification is based on a 5-class system (Plon et al., 2008). Benign (= class 1) variants are generally not reported.

2.2 | Droplet digital PCR

Droplet digital PCR (ddPCR) was performed on the Bio-Rad QX200 system (Bio-Rad Laboratories Inc, Hercules, California). Primers were custom designed by BioRad based on the Variant identified in NGS. Two negative controls were included with each experiment. Data were analyzed with QuantaSoft™ Analysis Pro (Bio-Rad).

2.3 | Multiplex ligation-dependent probe amplification

Multiplex ligation-dependent probe amplification (MLPA) analysis for the genes *TSC1* und *TSC2* was performed with the SALSA MLPA-Kit P124-C3 und P337-B1 (MRC-Holland) according to the respective standard protocols (www.mrcholland.com). SALSA MLPA-Kit P337-B1 for *TSC2* includes two probes for *PKD1* located in exons 30 and 40. MLPA analysis was added for patient 1 using the MRC-Holland MLPA-kits P351 and P352.

2.4 | Allele-specific PCR

Allele-specific PCR (ASO-PCR) was performed with oligonucleotides specifically amplifying genomic sequences containing the mutation c.3045delinsCA, resulting in a fragment of 263 bp. Two negative controls were included.

Forward Primer: GCCGTGCATGCGTTG.

Mutation specific reverse primer: CTCCAGGTGGAGGTTTTTTG.

Control reverse primer: GCTCCAGGTGGAGGTTTTTC.

2.5 | Sanger sequencing

Sanger sequencing was performed according to standard protocol. The peak areas of the affected sequence were compared to our statistical peak area, an average of the peak areas of eight controls. This method allows the confirmation of known aberrations at rather low variant allele frequencies.

3 | CLINICAL REPORT

3.1 | Patient 1

This 32-year-old male patient was referred for genetic *TSC1* and *TSC2* analysis because of his facial angiofibromas. His family history was normal, and he had two healthy sons; aged 2 years and 7 months. The dermatological examination revealed round, well-circumscribed, 1 mm in diameter, confluent papules, localized in the nasal and paranasal areas that appeared gradually at the beginning of the third decade (Figure 1a). He never had any developmental, intellectual, or neurological problems. Due to the clinical suspicion of TSC, a blood sample was taken, and other consultations and imaging studies were scheduled. Next generation sequencing (NGS) found no relevant variants in lymphocyte DNA. Abdominal ultrasound showed only low-grade fatty liver disease, while the kidneys were unremarkable of normal size and without cysts. Ophthalmologic examination gave evidence of a single retinal hamartoma in the right eye. T2-weighted cranial magnetic resonance imaging (cMRI) revealed several hyperintense cortical tubers and a space-occupying enhancing lesion from the ventricle ependyma in the left foramen of Monro, corresponding to a subependymal giant cell astrocytoma (SEGA). Based on this information, the clinical diagnosis of TSC became more likely and prompted further genetic analyses in fibroblasts from a biopsied facial angiofibroma and a normal skin sample. NGS of the angiofibroma DNA revealed the heterozygous *TSC2* mutation c.3045delinsCA (p.Asn1017Lysfs*151), which was confirmed by ASO-PCR (Figure 2a). In addition, MLPA displayed a deletion of the *TSC2*-gene along with the exons 30 and 40 of the *PKD1* gene in 40–60% of the analyzed cells. The unaffected skin fibroblasts showed an identical deletion in 30–50% of the cells (Figure 2b), while the *TSC2* mutation c.3045delinsCA could not be detected. Additional MLPA analysis showed that all exons of the *PKD1* gene were deleted to the same extent as the *TSC2* gene.

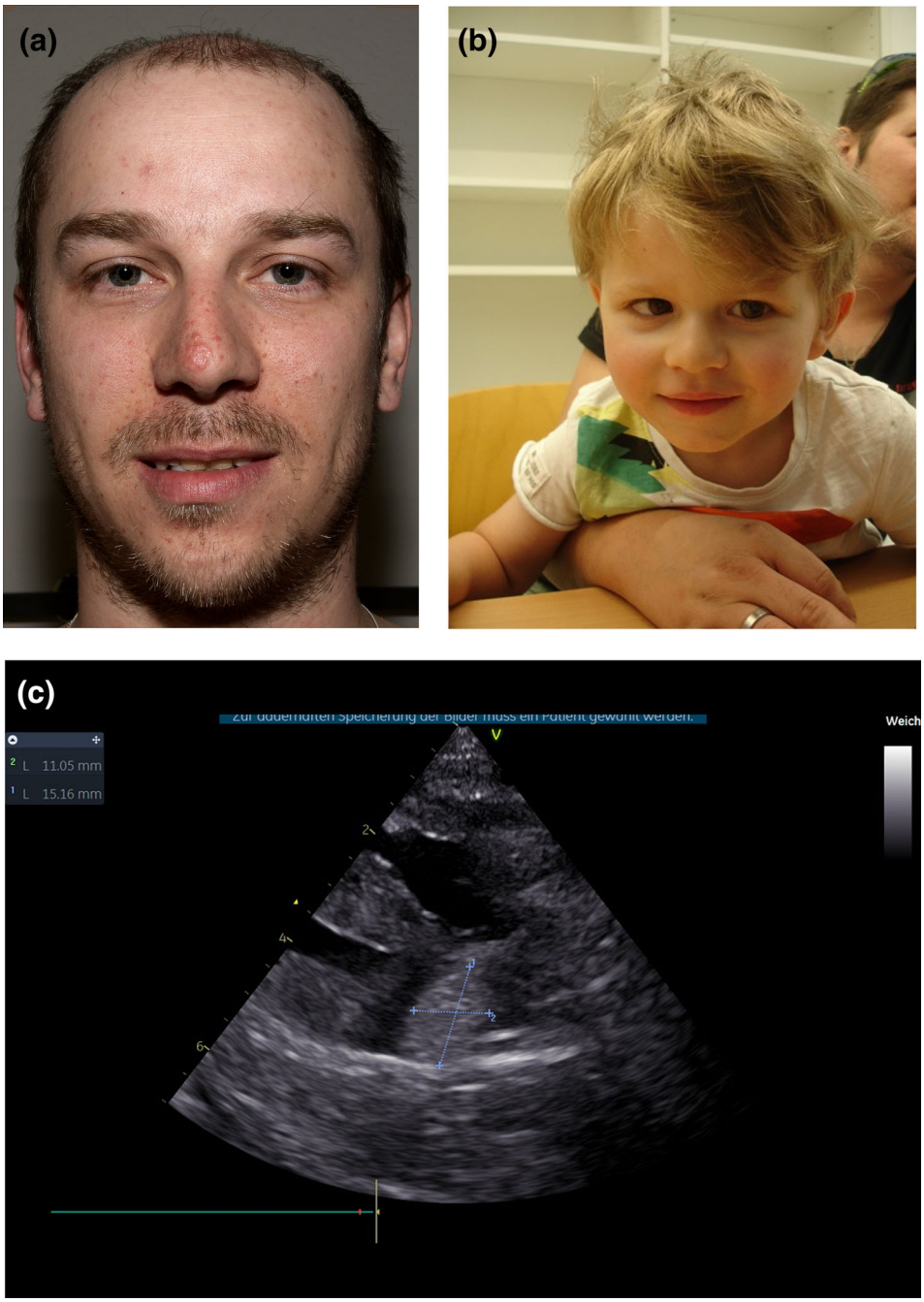

FIGURE 1 Clinical features of our patients. (a) Facial angiofibromas of patient 1. (b) Facial features of patient 2. (c) Echocardiogram at 2 weeks after delivery showing multiple rhabdomyomas in patient 3

Presently, it is not known if the renal tissue of the patient is affected by the deletion, monitoring of the kidneys is recommended. Somatic mosaicism of *PKD1/TSC2*-microdeletion (*contiguous-gene syndrome*) was established as the final molecular diagnosis.

3.2 | Patient 2

The proband was a 3-year-old Caucasian male (Figure 1b) with a longstanding previous medical history. He was the second of two children; the 6-year-old brother was healthy. Prenatal ultrasound revealed a cardiac rhabdomyoma and an arachnoid cyst at the 22nd week of gestation. The boy was delivered uneventfully at term but presented 3 weeks later with generalized epileptic seizures. Echocardiography confirmed two rhabdomyomas of 5 and 4.6 mm in diameter. Postnatal cMRI at 1 and 10 months of age gave evidence of a large parietooccipital arachnoid cyst of 6 cm, periventricular nodular heterotopia, and a cortical gyration abnormality. Psychomotor development was delayed; he walked at around 16–17 months and started to speak single words at 21 months. When last seen at age 3, the patient had a psychosocial delay of about 12 months, convergent strabismus of the right eye, and showed only poor social interaction. He had no dermatological lesion suspicious for TSC. First attempts to achieve a genetic diagnosis at 10 months of age included Sanger

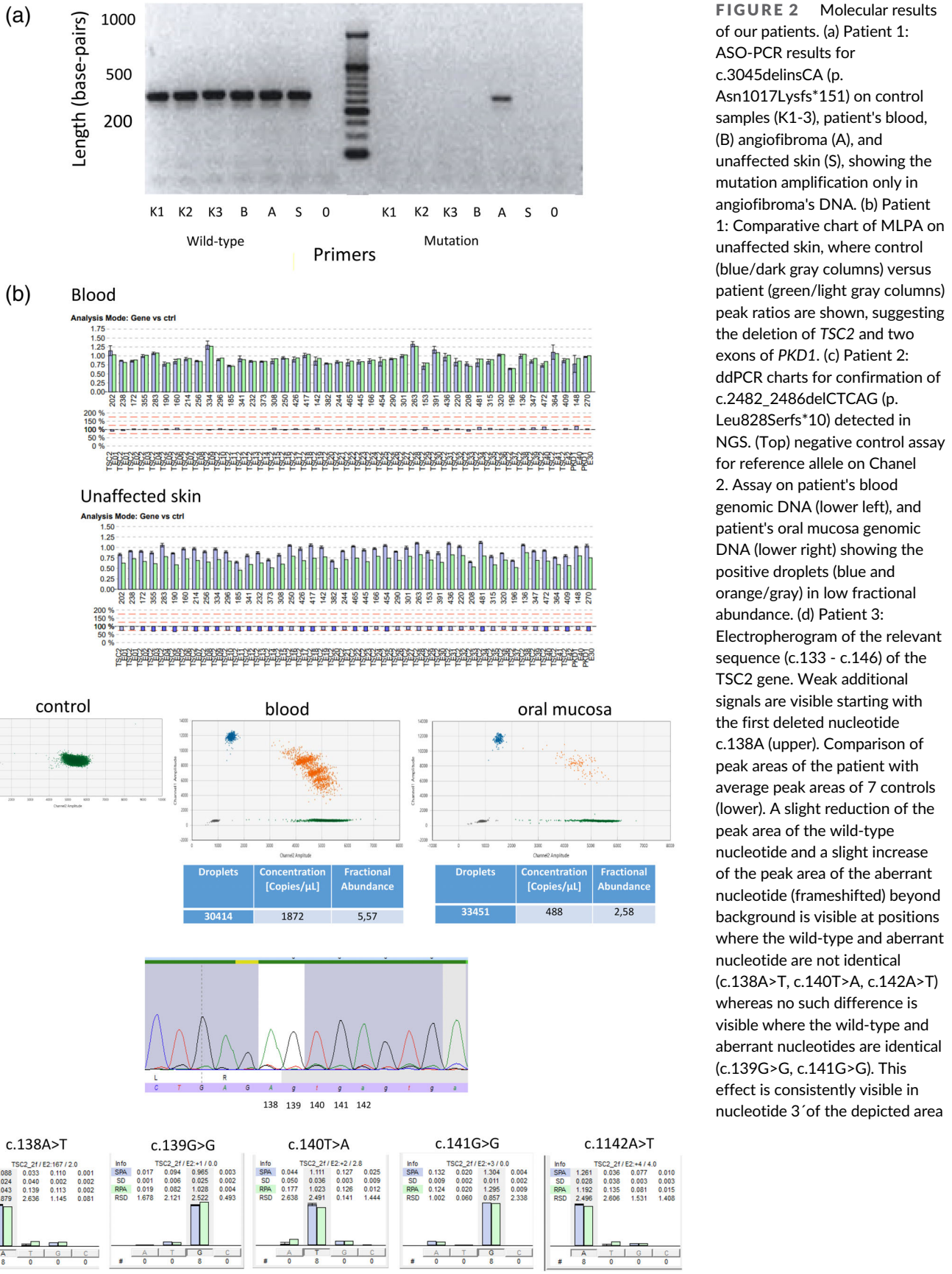

FIGURE 2 Molecular results of our patients. (a) Patient 1: ASO-PCR results for c.3045delinsCA (p. Asn1017Lysfs*151) on control samples (K1-3), patient's blood, (B) angiofibroma (A), and unaffected skin (S), showing the mutation amplification only in angiofibroma's DNA. (b) Patient 1: Comparative chart of MLPA on unaffected skin, where control (blue/dark gray columns) versus patient (green/light gray columns) peak ratios are shown, suggesting the deletion of *TSC2* and two exons of *PKD1*. (c) Patient 2: ddPCR charts for confirmation of c.2482_2486delCTCAG (p. Leu828Serfs*10) detected in NGS. (Top) negative control assay for reference allele on Chanel 2. Assay on patient's blood genomic DNA (lower left), and patient's oral mucosa genomic DNA (lower right) showing the positive droplets (blue and orange/gray) in low fractional abundance. (d) Patient 3: Electropherogram of the relevant sequence (c.133 - c.146) of the TSC2 gene. Weak additional signals are visible starting with the first deleted nucleotide c.138A (upper). Comparison of peak areas of the patient with average peak areas of 7 controls (lower). A slight reduction of the peak area of the wild-type nucleotide and a slight increase of the peak area of the aberrant nucleotide (frameshifted) beyond background is visible at positions where the wild-type and aberrant nucleotide are not identical (c.138A>T, c.140T>A, c.142A>T) whereas no such difference is visible where the wild-type and aberrant nucleotides are identical (c.139G>G, c.141G>G). This effect is consistently visible in nucleotide 3´of the depicted area

sequencing and MLPA of *TSC1* and *TSC2*. Results were normal; therefore, alternate diagnoses were suggested. As TSC remained the primary diagnostic target, we performed NGS of a new blood sample 2 years later. We found a 5-bp deletion c.2482_2486delCTCAG (p.Leu828Serfs*10) in the *TSC1* gene in approximately 4% of the reads, which corresponded to 8% of the blood leucocytes. The result was confirmed by means of ddPCR detecting the mutation in 5.6% of the sequences, corresponding to 10–12% of the cells. In addition, ddPCR in oral mucosa showed that approximately 5% of the cells carried the mutation (Figure 2c).

3.3 | Patient 3

The patient was a 9-month-old male infant. Prenatal history included intracardial masses, pneumothorax, diabetes-associated fetopathy with temporary hyperinsulinism, and persistent pulmonary hypertension. The child was born at 36 + 5 weeks of gestation via Cesarean section following pathological doppler findings. He was the second child of nonconsanguineous Caucasian parents. Two weeks after delivery, heart masses with the typical image of rhabdomyoma were observed by echocardiography (Figure 1c). In total, eight tumors ranging from 2.5 to 12.9 mm in diameter were detected. None of them implicated any cardiac inflow or outflow problem. Abdominal ultrasound and dermatological examinations were normal. Ophthalmological examination showed a single hamartoma of the left eye. One month after birth, cMRI disclosed subependymal and cortical hamartomas, and a lesion next to the foramen of Monro, 6 mm in diameter, corresponding to a SEGA. Neuropediatric examination revealed normal psychomotor development and a normal EEG. At 9 months of age, only one rhabdomyoma (0.5 cm) was still detectable. A new finding was a single angiomyolipoma of the left kidney 1 cm in diameter. NGS of a blood sample revealed a 2-bp-deletion c.138_138 + 1delAG (p.Glu47Thrfs*19) in 10% of the reads in *TSC2* corresponding to 20% affected blood lymphocytes. The result was confirmed by Sanger sequencing. *TSC1* analysis was normal.

3.4 | Patient 4

This boy was seen by geneticists for the first time at the age of 9 years due to facial and oral angiofibromas. Further physical examination revealed several hypopigmented macules; most of them located on the thorax with an average diameter of 1.5 cm. Ophthalmological examination of the left eye gave evidence of a single hamartoma. cMRI showed cortical dysplasias and subependymal nodules (SEN), and the abdominal ultrasound revealed multiple angiomyolipomas in both kidneys, which appeared progressively. Cognitive function was normal. Massive parallel sequencing of a blood sample revealed a nonsense mutation c.3581G > A (p.Trp1194*) in 5% of the reads in *TSC2*, corresponding to 10% affected blood lymphocytes, which was confirmed with ddPCR detecting the mutation in 4% of the sequences, corresponding to 8% of the cells.*TSC1* analysis was normal.

4 | DISCUSSION

Somatic mosaicism is often associated with a milder disease presentation in TSC (Treichel et al., 2019; Tyburczy et al., 2015). However, our clinical reports confirm the broad clinical variability of mosaic TSC even when detected as very low-level mosaicism in the tissues analyzed. This may be explained by the fact that the percentage of affected cells in a tissue analyzed does not allow conclusions on the proportion of affected cells in not analyzed tissues. From our series, the diagnosis of TSC in patient 1 remained unclear for almost a decade following his first dermatological manifestations. While in patient 2, the initial normal sequencing results of *TSC1* and *TSC2* led to the assumption of an alternate diagnosis for his epileptic encephalopathy. Similar diagnostic difficulties were previously reported (Byers et al., 2018). Our cases (summarized in Table 1) underline the relevance of a molecular methodology that is capable to detect very low-level *TSC1* and *TSC2* mosaicism in different tissues.

It is important to consider the age-related prevalence of clinical features. While cardiac rhabdomyoma is a specific pre- and postnatal feature of TSC and cortical tubers or dysplasias occur within the first 18 months of age (Davis et al., 2017), renal or pulmonary manifestations develop gradually over youth and early adulthood (Curatolo et al., 2008). Skin manifestations can generally be detected in the first year (hypomelanotic nodules); however, facial angiofibroma arise more slowly in the first decade. The age at first consultation in our cohort ranged from 9 months to 32 years. The patients had clinical manifestations in five different organs: heart, skin/mucosa, brain, eyes, and kidneys.

We identified five pathogenic mutations (Table 1), four of them in the *TSC2* gene. The *TSC2* mutations consisted of three truncating mutations and one large deletion, the only *TSC1* mutation was also a truncating mutation. By means of massive parallel sequencing low-level mutant allele frequencies (MAF) (≤10%) were detected in three out of four blood samples. The majority of mutations found in the *TSC1* and *TSC2* genes are point mutations and indels; this applies also to mosaicism (Tyburczy et al., 2015). MLPA is sensitive to detect large quantitative changes, however, NGS might achieve its performance in detection of large copy number variations ([CNV], with an extension of at least 1 Kb DNA) in addition to a better sensitivity for indels and point mutations (Ismail et al., 2017; Kerkhof et al., 2017). Consequently, NGS technologies are gradually becoming a feasible option in diagnosis for inconclusive TSC cases (Treichel et al., 2020).

A venous blood sample is normally the first tissue to obtain DNA for genetic analysis. However, in mosaicism for TSC, the mutational load is higher in affected tissues in comparison to peripheral blood. If present, facial angiofibroma is easily accessible and suitable for genetic analysis when TSC mosaicism is suspected (Giannikou et al., 2019). We analyzed samples from various tissues to identify the disease cause or to validate and quantify the previously identified

TABLE 1 Clinical and laboratory summary of our patients

Subject	Age	Sex	Major features	Organ affected					No. of attempts	Molecular technique	Type of sample	Affected gene	Mutation	MAF (%)
				H	S	B	E	K						
Patient 1	32 years	Male	AF; CD; SEGA; RH (single)	N	Y	Y	Y	N	1.	Next Generation Sequencing	Blood	Normal	—	—
									2.	MLPA	Blood	Normal	—	—
									3.	Next Generation Sequencing	Unaffected skin	*TSC2*	deletion	—
											Angiofibroma	*TSC2*	c.3045delinsCA	4.4
										MLPA	Unaffected skin	*TSC2/ PKD1*	deletion	15–25
											Angiofibroma	*TSC2/ PKD1*	deletion	20–30
										ASO-PCR	Blood	Normal	—	—
											Unaffected skin	Normal	—	—
											Angiofibroma	*TSC2*	c.3045delinsCA	—
Patient 2	3 years	Male	CR	Y	N	Y	N	N	1.	Sanger	Blood	Normal	—	—
										MLPA	Blood	Normal	—	—
									2.	Next Generation Sequencing	Blood	*TSC1*	c.2482_2486delCTCAG	4
									3.	ddPCR	Blood	*TSC1*	c.2482_2486delCTCAG	5.6
											Oral mucosa	*TSC1*	c.2482_2486delCTCAG	2.6
Patient 3	9 months	Male	CR; CD; SEGA; SN; RH (single); AML (single)	Y	N	Y	Y	Y	1.	Next Generation Sequencing	Blood	*TSC2*	c.138_138 + 1delAG	10
										Sanger	Blood	*TSC2*	c.138_138 + 1delAG	10
Patient 4	9 years	Male	AF; HM; CD; SN; RH (single); AML	N	Y	Y	Y	Y	1.	Next Generation Sequencing	Blood	*TSC2*	c.3581G > A	5
										ddPCR	Blood	*TSC2*	c.3581G > A	4

Abbreviations: AF, angiofibromas; AML, angiomyolipomas; ASO-PCR, allele-specific oligonucleotide polymerase chain reaction B: brain; CD, cortical dysplasia; CR, cardiac rhabdomyoma; ddPCR, droplet digital polymerase chain reaction; E, eye; H, heart; HM, hypomelanotic macules; K, kidney; MAF, mutant allele frequency; MLPA, multiple ligation-dependent probe amplification; N, no; RH, retinal hamartomas; S, skin; SEGA, subependymal giant cell astrocytoma; SN, subependymal nodules; Y, yes.

mutations. In patient 1, the first analysis from blood using MLPA showed no mutation, but the same method applied on affected and unaffected skin biopsy permitted to find the deletion responsible for *TSC2/PKD1* contiguous gene syndrome. In patient 1, nonquantitative allele-specific-oligo PCR (ASO-PCR) was applied to assess the *TSC2* point mutation in different tissues (Table 1). The absence of the mutation in blood and healthy skin confirmed that the mutation identified by NGS in the angiofibroma of patient 1 was indeed a second-hit mutation. This is consistent with previous outcomes, in which most of the second-hit mutations in skin lesions from TSC patients are indels or point mutations (Tyburczy et al., 2014). ASO PCR can confirm low-level mosaicism already identified by NGS techniques, and has shown better sensitivity than Sanger sequencing for this purpose (Nellist et al., 2015).

To conclude, we recommend the use of NGS techniques as a standard first tier method for *TSC1* and *TSC2* testing, provided that a high sequence coverage is achieved. In addition, NGS also allows the detection of CNV with a lower sensitivity. For the detection of CNV, the use of MLPA still is the standard method. However, the increasing availability and cost effectiveness of SNP arrays may challenge this position in the future. To confirm point mutations or indels, the method of choice is ddPCR, which is very sensitive and highly quantitative. However, ddPCR may not be available in every laboratory. ASO-PCR has a similar sensitivity as ddPCR; however, does not allow any quantification. Sanger sequencing is not useful for mosaicism detection due to its low sensitivity and poor quantification ability.

The correct molecular identification of TSC is important for outcome prediction and therapeutic options. Three of our patients presented focal cortical dysplasia and one of them had seizures and generalized neurocognitive disorder. A genetic diagnosis may be significant for prompt interventions in seizures for patients with clinical suspicion of TSC (Słowińska et al., 2018). *TSC2/PKD1* microdeletion as found in patient 1 has a well-known genotype–phenotype correlation, whereby regular imaging and functional monitoring of kidneys is recommended (Sampson et al., 1997). The discovery of mTOR pathway upregulation in tuberous-sclerosis-associated tumors presents new possibilities for treatment strategies. Moreover, the molecular diagnosis allows genetic counseling of patients and parents for reproductive options. The recurrence risk to siblings is not increased in mosaic TSC; however, there is a risk of transmission to offspring, since gonadal involvement in our patients cannot be excluded.

ACKNOWLEDGMENT

The authors would like to thank the patients and their families for their consent to have their data and pictures published.

CONFLICT OF INTEREST

The authors have no conflict of interest to declare.

DATA AVAILABILITY STATEMENT

The data are not publicly available due to privacy or ethical restrictions.

ORCID

Sabine Rudnik-Schöneborn https://orcid.org/0000-0001-8332-0672

REFERENCES

Byers, H. M., Jensen, D. M., Glass, I. A., & Bennett, J. T. (2018). Minimal mosaicism, maximal phenotype: Discordance between clinical and molecular findings in two patients with tuberous sclerosis. *American Journal of Medical Genetics, Part C: Seminars in Medical Genetics*, *178*(3), 374–378. https://doi.org/10.1002/ajmg.c.31656

Curatolo, P., Bombardieri, R., & Jozwiak, S. (2008). Tuberous sclerosis. In *The Lancet* (Vol. 372, Issue 9639), (pp. 657–668). Elsevier B.V.

Davis, P. E., Filip-Dhima, R., Sideridis, G., Peters, J. M., Au, K. S., Northrup, H., Bebin, E. M., Wu, J. Y., Krueger, D., Sahin, M., Warfield, S., Scherrer, B., Goyal, M., Dies, K., Bruns, S., Hanson, E., Walsh, A., Bing, N., Kent, B., … Leuchter, A. (2017). Presentation and diagnosis of tuberous sclerosis complex in infants. *Pediatrics*, *140*(6), 1–11. https://doi.org/10.1542/peds.2016-4040

den Dunnen, J. T., & Antonarakis, E. (2001). Nomenclature for the description of human sequence variations. *Human Genetics*, *109*, 121–124. https://doi.org/10.1007/s004390100505

Giannikou, K., Lasseter, K. D., Grevelink, J. M., Tyburczy, M. E., Dies, K. A., Zhu, Z., Hamieh, L., Wollison, B. M., Thorner, A. R., Ruoss, S. J., Thiele, E. A., Sahin, M., & Kwiatkowski, D. J. (2019). Low-level mosaicism in tuberous sclerosis complex: Prevalence, clinical features, and risk of disease transmission. *Genetics in Medicine*, *21*(11), 2639–2643. https://doi.org/10.1038/s41436-019-0562-6

Ismail, N. F. D., Rani, A. Q., Nik Abdul Malik, N. M. A., Boon Hock, C., Mohd Azlan, S. N., Abdul Razak, S., Keng, W. T., Ngu, L. H., Silawati, A. R., Yahya, N. A., Mohd Yusoff, N., Sasongko, T. H., & Zabidi-Hussin, Z. A. M. H. (2017). Combination of multiple ligation-dependent probe amplification and Illumina MiSeq amplicon sequencing for TSC1/TSC2 gene analyses in patients with tuberous sclerosis complex. *Journal of Molecular Diagnostics*, *19*(2), 265–276. https://doi.org/10.1016/j.jmoldx.2016.10.009

Kerkhof, J., Schenkel, L. C., Reilly, J., McRobbie, S., Aref-Eshghi, E., Stuart, A., Rupar, C. A., Adams, P., Hegele, R. A., Lin, H., Rodenhiser, D., Knoll, J., Ainsworth, P. J., & Sadikovic, B. (2017). Clinical validation of copy number variant detection from targeted next-generation sequencing panels. *Journal of Molecular Diagnostics*, *19*(6), 905–920. https://doi.org/10.1016/j.jmoldx.2017.07.004

Nellist, M., Brouwer, R. W. W., Kockx, C. E. M., van Veghel-Plandsoen, M., Withagen-Hermans, C., Prins-Bakker, L., Hoogeveen-Westerveld, M., Mrsic, A., van den Berg, M. M. P., Koopmans, A. E., de Wit, M. C., Jansen, F. E., Maat-Kievit, A. J. A., van den Ouweland, A., Halley, D., de Klein, A., & van IJcken, W. F. J. (2015). Targeted next generation sequencing reveals previously unidentified and mutations. *BMC Medical Genetics*, *16*(1), 1–11. https://doi.org/10.1186/s12881-015-0155-4

Plon, S. E., Eccles, D. M., Easton, D., Foulkes, W. D., Genuardi, M., Greenblatt, M. S., Hogervorst, F. B. L., Hoogerbrugge, N., Spurdle, A. B., & Tavtigian, S. (2008). Sequence variant classification and reporting: Recommendations for improving the interpretation of cancer susceptibility genetic test results. *Human Mutation*, *29*(11), 1282–1291. https://doi.org/10.1002/humu.20880

Povysil, G., Tzika, A., Vogt, J., Haunschmid, V., Messiaen, L., Zschocke, J., Klambauer, G., Hochreiter, S., & Wimmer, K. (2017). Panelcn.MOPS: Copy-number detection in targeted NGS panel data for clinical diagnostics. *Human Mutation*, *2017*(38), 889–897. https://doi.org/10.1002/humu.23237

Sampson, J. R., Maheshwar, M. M., Aspinwall, R., Thompson, P., Cheadle, J. P., Ravine, D., Roy, S., Haan, E., Bernstein, J., & Harris, P. C.

(1997). Renal cystic disease in tuberous sclerosis: Role of the polycystic kidney disease 1 gene. *American Journal of Human Genetics*, *61*(4), 843–851. https://doi.org/10.1086/514888

Słowińska, M., Jóźwiak, S., Peron, A., Borkowska, J., Chmielewski, D., Sadowski, K., Jurkiewicz, E., Vignoli, A., La Briola, F., Canevini, M. P., & Kotulska-Jóźwiak, K. (2018). Early diagnosis of tuberous sclerosis complex: A race against time. How to make the diagnosis before seizures? *Orphanet Journal of Rare Diseases*, *13*(1), 1–10. https://doi.org/10.1186/s13023-018-0764-z

Treichel, A. M., Kwiatkowski, D. J., Moss, J., & Darling, T. N. (2020). A diagnostic algorithm for enhanced detection of mosaic tuberous sclerosis complex in adults. *British Journal of Dermatology*, *182*(1), 235–237. https://doi.org/10.1111/bjd.18332

Treichel, Alison M., Hamieh, L., Nathan, N. R., Tyburczy, M. E., Wang, J. an, Oyerinde, O., Raiciulescu, S., Julien-Williams, P., Jones, A. M., Gopalakrishnan, V., Moss, J., Kwiatkowski, D. J., & Darling, T. N. (2019). Phenotypic distinctions between mosaic forms of tuberous sclerosis complex. *Genetics in Medicine*, *21*(11), 2594–2604. https://doi.org/10.1038/s41436-019-0520-3

Tyburczy, M. E., Dies, K. A., Glass, J., Camposano, S., Chekaluk, Y., Thorner, A. R., Lin, L., Krueger, D., Franz, D. N., Thiele, E. A., Sahin, M., & Kwiatkowski, D. J. (2015). Mosaic and Intronic mutations in TSC1/TSC2 explain the majority of TSC patients with no mutation identified by conventional testing. *PLoS Genetics*, *11*(11), 1–17. https://doi.org/10.1371/journal.pgen.1005637.

Tyburczy, M. E., Wang, J. A., Li, S., Thangapazham, R., Chekaluk, Y., Moss, J., Kwiatkowski, D. J., & Darling, T. N. (2014). Sun exposure causes somatic second-hit mutations and angiofibroma development in tuberous sclerosis complex. *Human Molecular Genetics*, *23*(8), 2023–2029. https://doi.org/10.1093/hmg/ddt597

How to cite this article: Manzanilla-Romero, H. H., Weis, D., Schnaiter, S., & Rudnik-Schöneborn, S. (2021). Low-level mosaicism in tuberous sclerosis complex in four unrelated patients: Comparison of clinical characteristics and diagnostic pathways. *American Journal of Medical Genetics Part A*, *185*A: 3851–3858. https://doi.org/10.1002/ajmg.a.62433